Transactions of the Materials Research Society of Japan 29[7] 3017-3020 (2004)

Shape Memory Characteristics of Ti-Nb-Ge Alloy

Yusuke Fukui[+], Tomonari Inamura, Hideki Hosoda[++], Kenji Wakashima and Shuichi Miyazaki[*]

Precision and Intelligence Laboratory (P&I Lab), Tokyo Institute of Technology (Tokyo Tech)
4259 Nagatsuta, Midori-ku, Yokohama 226-8503, Japan
Phone&Fax: 81-45-924-5057, Email: hosoda@pi.titech.ac.jp ([++]corresponding author)
[*]Institute of Material Science, University of Tsukuba, Tennodai 1-1-1, Tsukuba, Ibaraki 305-8573, Japan,
Phone&Fax: 81-298-53-5283, Email: miyazaki@ims.tsukuba.ac.jp
[+]Graduate student, Tokyo Institute of Technology
Phone&Fax: 81-45-924-5061, Email: fukui@ken.pi.titech.ac.jp

Abstract

Mechanical and shape memory properties of a Ti-Nb-Ge alloy were investigated, which are expected for biomedical and functional applications in order to replace Ti-Ni shape memory alloys. The Ti-Nb-Ge alloy was fabricated by Ar arc melting method by a homogenization at 1273K for 7.2ks and then cold-rolled with the reduction of 99% in thickness without intermediate annealing. Some of the cold rolled plates were solution-treated at 1273K for 1.8ks after the cold-rolling. Then, X-ray diffraction (XRD) pole figure measurements were done using $\{110\}_\beta$ reflection from the bcc parent phase (β). Besides, cyclic loading-unloading tensile tests were carried out in a temperature range from 193K to room temperature (RT). The results of XRD pole figure measurements suggest that well-developed textures are formed for both the cold-rolled and the solution-treated specimens, and that the former is a deformation texture and the latter is a recrystallized texture. Besides, the tensile tests revealed that the solution-treated specimens exhibit superelasticity, and the superelastic stain due to the stress-induced martensitic transformation increases with increasing the number of loading-unloading deformation cycles. Therefore, this alloy is hopeful to be a practical biomedical shape memory alloy.

Key words: shape memory alloy, Ti-Nb-Ge, X-ray diffraction pole figure, texture, superelasticity

1. Introduction

Recently, the biomedical applications such as stents and gidewires of shape memory alloys (SMAs) become widely day by day, and the practical SMAs commonly used are Ti-Ni. However, the possibility of Ni-hypersensitivity is pointed out for the Ti-Ni. Then, Ni-free Ti-base SMAs composed of non-toxic elements are strongly required. Based on such background, our group has a systematic work for developing new titanium-base nontoxic SMAs [1-13]. These Ti-base SMAs composed of nontoxic elements have a disordered bcc crystal structure of the austenite phase (β), and a *c*-centered orthorhombic cell of the martensite phase (α") [14]. The mechanical properties of these alloys are: ultimate tensile strength of 600-1000MPa, fracture strain of 10-40% and Young's modulus of 30-60GPa. The details are described in the references. Quite recently, we have studied for TiNbAl [8-13] and TiNbGe alloys [8] and found that TiNbAl exhibited superior superelasticity and large anisotropy due to textures developed during the processing. On the other hand, superelastic behavior and crystallographic investigation for TiNbGe were not studied yet. Then, the purpose of this study is to clarify the superelastic behavior and crystallographic features of Ti-24mol%Nb-3mol%Ge (abbreviated as Ti24Nb3Ge, hereafter).

2. Experimental procedure

The nominal composition of the Ni-free Ti-base SMA investigated was chosen to be Ti-24mol%Nb-3mol%Ge, and the alloy is called Ti24Nb3Ge, hereafter. The alloy was prepared by Ar arc melting method using high purity elemental Ti (99.99%), Nb (99.99%) and Ge (99.99%). The ingot was homogenized at 1273K for 7.2ks in vacuum, and then cold-rolled to be 99% reduction in thickness (0.1mm in thickness). After the cold rolling, some pieces of plates were solution-treated at 1273K for 1.8ks in vacuum followed by quenching into water. The specimens are called Ti24Nb3Ge-CW and Ti24Nb3Ge-ST where CW and ST stand for the cold work and the solution treatment, respectively.

X-ray diffraction (XRD) pole-figure measurement was done by a Philips X'Pert PRO MRD system XRD pole figures were obtained using the {110} reflection from the bcc austenite phase (β) where CuKα was and a graphite monochrometer were used. Superelastic properties were evaluated through cyclic loading-unloading tensile tests performed in a temperature range from 193K to RT under a strain rate of 5×10^{-4}/s and a constant strain increment of 1% per loading-unloading cycle using Shimadzu Autograph

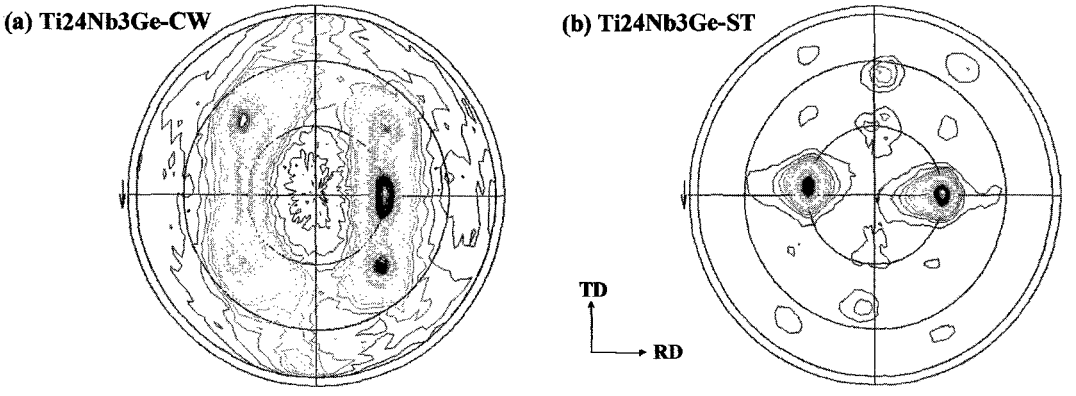

Figure 1 XRD pole figures taken from {110} reflections of bcc phase: (a) Ti24Nb3Ge-CW and (b) Ti24Nb3Ge-ST

500NI. In the tensile tests the tensile axis of specimens was chosen to be the rolling direction (RD). The specimens with a gauge length of 10mm were made by cut and damaged surface was removed by polishing.

3. Results and discussion

3.1 XRD pole figures

Figure 1 shows XRD pole figures taken from $\{110\}_\beta$ reflection: (a) Ti24Nb3Ge-CW and (b) Ti24Nb3Ge-ST. It should be noted that, regardless of cold-rolling reduction and heat treatment condition, the apparent phase at RT is the bcc phase, not the martensitic α" phase. Dark and dense area in the pole figure corresponds to high intensity of XRD reflection. It is found that (1) both cold-rolled and solution-treated specimens exhibit textures, (2) the texture type formed after the solution treatment is different from that formed by the cold rolling. The texture after the cold rolling is a deformation texture and the surface plane is {100} and the rolling direction is <110>. On the other hand, the texture after the solution treatment is a recrystallization texture and the surface plane is {112} and the rolling direction is <110>. Further details of the textures and texture development are now being investigated by means of orientation distribution functions.

3.2 Tensile tests

(a) Stress-strain curves

Figure 2 shows stress-strain curves obtained by the constant strain increment tests for Ti24Nb3Ge at (a) RT and at (b) 193K. In these experiments, the specimens were firstly deformed up to 1% strain and unloaded. Then, the specimens were again loaded up to 2% (previous strain of 1% plus additional strain increment of 1% constant) strain and unloaded. And the specimens were also deformed again up to 3% (=2%+1%) strain and unloaded. Such cyclic loading-unloading deformation was repeated up to 10% in total strain.

It is clear in Fig. 2 that the alloy exhibits some superelasticity at both RT and 193K and that the superelasticity is much clear at 193K than at RT. The clear superelasticity seen at 193K is probably due to higher critical stress for dislocation slip: Pierls stress in general bcc metals and alloys largely increase with decreasing temperature. Then, with decreasing temperature, stress induced martensitic transformation becomes a dominant mechanism for deformation in comparison with dislocation slip. In actual, the residual strain after tensile tests is 6.5% at RT and this value is lager than 5.0% at 193K. Larger permanent strain remained at higher test temperature. Therefore, superelasticity becomes better with decreasing temperature.

In our previous work for Ti-24mol%Nb-3mol%Al alloy (abbreviated as Ti24N3Al), it was reported that similar and well-developed textures were also formed after the cold-rolling and the solution treatment and that superelasticity strongly depended on the tensile direction [12]. Then, similar anisotropic superelasticity should appear in the cases of Ti24Nb3Al as well as Ti24Nb3Al. The dependence of superelasticity on tensile direction is now being investigated.

(b) Clausius-Clapeyron relationship

Figure 3 shows the stress to induce martensitic transformation (σ_{SIMT}) as a function of test temperature. Here, σ_{SIMT} is 0.2% flow stress in the first loading-unloading cycles. It was found that σ_{SIMT} decreases linearly with decreasing test temperature. This linear relationship is known to be Clausius-Clapeyron relationship and the slope is estimated to be 1.1MPa/K. Based on this relationship, the martensitic transformation start temperature (M_s) under the zero pressure is evaluated to be 60K by extrapolation. The 60K of M_s is quite low in comparison with 201K of M_s in Ti24Nb3Al [13]. This result suggests that the ternary element Ge significantly reduces M_s in the Ti-Nb alloys.

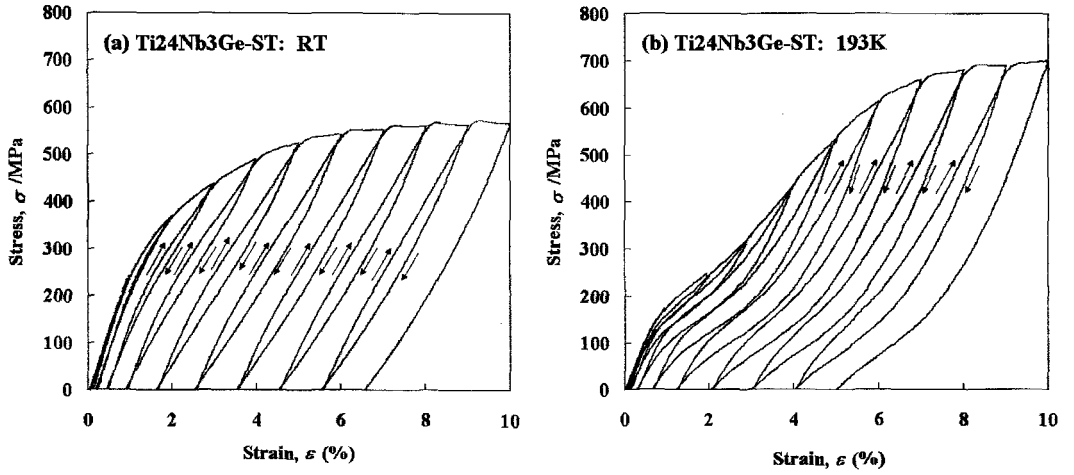

Figure 2 Selected stress-strain curves obtained by cyclic loading-unloading tensile tests for Ti24Nb3Ge-ST at (a) RT and (b) 193K. It is noted that pseudoelasticity appears at both test temperatures, and that the pseudoelastic strain by unloading is larger at 193K.

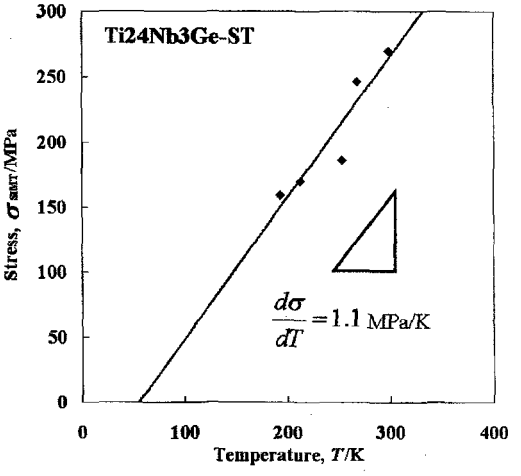

Figure 3 Temperature dependence of stress to induce martensitic transformation in Ti24Nb3Ge-ST.

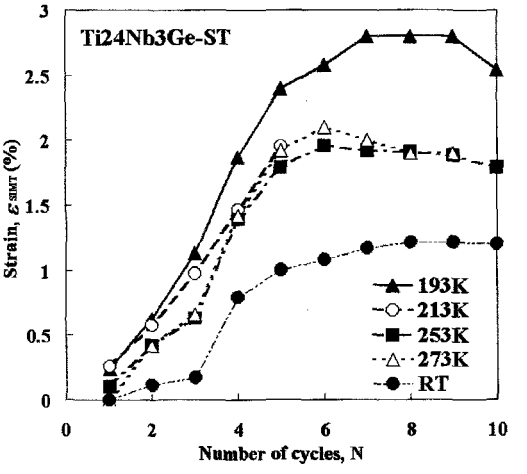

Figure 4 Effect of the number of cyclic deformation on superelastic strain (ε_{SIMT}) Ti24Nb3Ge-ST tested at various temperatures.

(c) Effect of cyclic deformation

The effect of cyclic deformation on superelasticity in each loading-unloading cycle is drawn in Figure 4. It is clear that the superelastic strain (ε_{SIMT}) becomes larger with decreasing test temperature after a same number of deformation cycles. This is due to temperature dependence of critical stress for slip as mentioned previously.

Besides, ε_{SIMT} increases with increasing the number of cycles. With further increasing the number of cycles, however, ε_{SIMT} becomes constant or decreases slightly. Such phenomena can be explained as follows. (1) With increasing the number of cycles, work hardening occurs due to the accumulation of dislocations. (2) Then, critical stress for slip increases by work hardening. (3) As a result, stress-induced martensitic transformation becomes stable by the work hardening in a similar manner by lowering temperature. The maximum superelastic strain is 2.8% at 193K and 1.2% at RT. When the amount of plastic deformation exceeds a

certain limit, the martensitic transformation is prevented by a large amount of dislocations and then the superelasticity becomes decreasing. Similar phenomena were also observed in Ti24Nb3Al [13] as well as general shape memory alloys.

4. Conclusions

By using two kinds of cold-worked (CW) and solution-treated (ST) Ti24Nb3Ge biomedical shape memory alloys (Ti24Nb3Ge-CW, Ti24Nb3Ge-ST), the XRD pole figure measurement and cyclic loading-unloading tensile tests were performed and the conclusions are obtained as follows.

① Ti24Nb3Ge-CW exhibits a deformation texture. The surface plane is {100} and the rolling direction is <110>.

② Ti24Nb3Ge-ST exhibits a recrystallization texture. The surface plane is {112} and the rolling direction is <110>.

③ Martensitic transformation start temperature (M_s) of Ti24Nb3Ge-ST is evaluated to be 60K and the slope of Clausius-Clapeyron relationship of this alloy is estimated to be 1.1MPa/K.

④ Largest superelastic strain of Ti24Nb3Ge-ST reaches 2.8% at 193K and 1.2% at RT.

⑤ The strain caused by stress-induced martensitic transformation (ε_{SIMT}) depends on the number of loading-unloading cycles of the constant strain increment test, i.e., depends on the amount of the accumulated plastic deformation introduced by slip.

5. Acknowledgements

This work was partially supported by Furukawa Techno Material Co. Ltd., the 21st COE Program from the Ministry of Education, Culture, Sports, Science and Technology, Japan, and Osawa Scientific Studies Grants Foundation. The authors would like to thank Prof. H. Ishihara and Prof. H. Funakubo and Mr. M. Suzuki in Tokyo Institute of Technology for XRD pole figure measurements.

6. References

[1] H. Tada, H. Hosoda, M. Takeuchi, K. Hamada, K. Mizuuchi, K. Aoki and K. Inoue, The Third Pacific Rim International Conference on Advanced Materials and Processing (PRICM3), eds. M. A. Imam et al., TMS, 2, 1998, 3086.

[2] K. Inoue, K. Enami, K. Inoue, H. Tada, H. Hosoda and K. Hamada, Proc. Fourth Intl. Conf. on Intelligent Materials (ICIM'98), eds. T. Takagi et al, Intelligent Materials Forum & The Society of Non-Traditional Technology, Science and Technology Agency, 1998, 88.

[3] H. Hosoda and S. Miyazaki, Intl. Workshop on Bio-integrated Materials & Tissue Engineering, NAIR, 2000, 26.

[4] H. Hosoda, Y. Ohmatsu and S. Miyazaki, Trans. MRS-J, 26, 2001, 235.

[5] H. Hosoda, N. Hosoda and S. Miyazaki, Trans. MRS-J, 26, 2001, 243.

[6] Y. Ohmatsu, H. Hosoda and S. Miyazaki, The Fourth Pacific Rim International Conference on Advanced Materials and Processing (PRICM4), eds. S. Hanada et al., The Japan Inst. Metals, 2, 2001, 1627.

[7] N. Hosoda, H. Hosoda and S. Miyazaki, The Fourth Pacific Rim International Conference on Advanced Materials and Processing (PRICM4), eds. S. Hanada et al., The Japan Inst. Metals, 2, 2001, 1623.

[8] K. Kuroda, H. Hosoda, K. Wakashima and S. Miyazaki, Trans. MRS-J, 28, [3] 2003, 631-634.

[9] Y. Fukui, K. Kuroda, H. Hosoda, K. Wakashima and S. Miyazaki, Trans. MRS-J, 28, [3] 2003, 623-626.

[10] H. Hosoda, Y. Fukui, T. Inamura, K. Wakashima, S. Miyazaki and K. Inoue, Mat. Sci. Forum, 426-432 2003, 3121-3126.

[11] T. Inamura, Y. Fukui, H. Hosoda, K. Wakashima and S. Miyazaki, Proc. of the 10th World Conf. on Titanium, (Eds: G. Lütjering), Wiley-VCH, in press.

[12] H. Hosoda, Y. Fukui, T. Inamura, K. Wakashima and S. Miyazaki, Proc. of the 10th World Conf. on Titanium, (Eds: G. Lütjering), Wiley-VCH, in press.

[13] Y. Fukui, T. Inamura, H. Hosoda, K. Wakashima and S. Miyazaki, Mater. Trans. in press.

[14] A. R. G. Brown, D. Clark, J. Eastbrook and K. S. Jepson, Nature, 4922, 1964, 914.

(Received October 10, 2003; Accepted March 20, 2004)